



Identification of erosion-prone areas using morphometric parameters, land use land cover and multi-criteria decision-making method: geo-informatics approach

Paolenmang Haokip¹ · Md. Abdullah Khan¹ · Pandurang Choudhari² ·
Luc Cimusa Kulimushi³ · Ibodullo Qaraev⁴

Received: 17 September 2020 / Accepted: 18 April 2021 / Published online: 4 May 2021
© The Author(s), under exclusive licence to Springer Nature B.V. 2021

Abstract

Soil erosion is the main driving force of several devastating natural hazards in the complex mountainous terrain of the Himalayas where the Teesta River basin is located. The present study focused on GIS-based multi-criteria analytical approach (MCA) that integrates morphometric parameters with land cover categories for identification of erosion hotspot areas through sub-watersheds prioritization. The general character of the eight sub-watersheds was derived from the linear, areal and relief aspects, while seven land cover types derived from maximum likelihood classification were evaluated in the MCA. Before combination of the studied parameters in MCA, each parameter was individually ranked and compound value (Cp) was calculated which produced four classes: low, medium, high and very high priority. Later, these ranks were integrated into MCA to give eight major classes classified from 1 to 8. Lowest Cp ranked 1 gets very high priority, while the highest Cp is ranked 8, i.e., lowest priority. The results revealed a predominance of dense forest account for 31.73% of the total area, the basin is a sixth-order river dominated by high relief and marginal slope, elongated in shape, and mean bifurcation ratio (Rb) was 3.879 which indicates an undistorted natural drainage system. Final MCA priority ranking indicated that: SW-4 and 5 having lowest Cp values (3.39 and 4) ranked 1 and 2 suggest very high erosion susceptibility, SW-8 and 3 (4.22 and 4.39) rated 3 and 4, i.e., high priority; SW-6 and 7 ranked 5 and 6, i.e., medium priority; and SW-1 and SW-2 ranked 7 and 8 because of their highest Cp (5.39 and 5.67), i.e., least priority. The prioritization result identified critical areas that are indispensable for sustainable use and management of water and land resources.

Keywords Morphometry · Land cover · Erosion susceptibility · Middle and Lower Teesta River basin · Geographic information system · Remote sensing · Sikkim

✉ Pandurang Choudhari
choudharipp79@gmail.com

Extended author information available on the last page of the article

1 Introduction

The survival of living systems on earth mainly depends on land and water resources. These resources are interdependent and interacting in various phases of their respective cycles. The well-being of the people, environment preservation and sustained food security depend on sustainable management of natural resources (Borkar et al., 2018).

However, lack of management and careless use of natural resources led to degradation and hence may become a major concern to the decision makers, researchers and planners (Kulimushi et al., 2021). Soil erosion among other forms of land degradation causes onsite loss of soil productivity and offsite water pollution, filling of riverbed and downstream flooding (Sharma et al., 2015; Uwemeye et al., 2020). Soil erosion is then a worldwide major agricultural and environmental problem (Morgan, 2009). The complex mountainous terrain of the Himalayas is an unstable and fragile ecosystem threatened by major driving force of several devastating natural hazards including the soil erosion due to resources overexploitation from anthropogenic activities added to the climate change (Chauhan et al., 2016; Huggel, 2004).

Consequently, adoption of better management needs to preserve the equilibrium between water and land on the one hand and human activities and land use on the other hand (Choudhari et al., 2018; Kolekar, 2021).

Soil loss susceptibility assessment focusing on key characteristics is hence important to maintain the level of soil productivity and hence reduce devastating consequences to the biophysical and socioeconomic, and environment (Kulimushi et al., 2021). Over the past decades, many approaches were taken to assess the soil erosion susceptibility, some involved the rainfall intensity, land cover, soil properties and topographic as the main triggering factors (Kavian et al., 2014; Rushema et al., 2020). Several authors including (Miller, 1953; Horton, 1945; Sreedevi et al., 2009) show that the main determinant of running water systems functioning at basin scale is the physical characteristics such as geology, lithology, soil, geomorphology, topography, vegetation and climate.

These physical parameters are interrelated and can be deeply understood through morphometric study to characterize a River basin, thus provide general information about hydrogeological behavior of a drainage basin such as stream order, density and frequency, length of overland flow, relief and channel slope together with other basin morphological aspects (Fenta et al., 2017). Furthermore, land cover is one of the most sensitive indicators of the interactions between human activities and the natural environment (Alkharabsheh et al., 2013). The same author shows that geomorphic conditions of the area associated with land cover patterns have an accelerating impact of the land degradation, therefore becoming useful elements to identify erosion prone areas. In doing so, computer-aided mapping (GIS and remote sensing) techniques become the most important progress in natural science (Chaubey et al., 2020). The GIS technology provides suitable alternatives for the efficient management of large and complex databases, while satellite remote sensing can obtain a synoptic view of a large area at one time and very useful for land, cover dynamics and morphometric study (Grohmann, 2004).

Some of the recent studies from different parts of the sphere have applied GIS in drainage characteristics studies for watershed prioritization using different methods such as Nitheshnirmal et al., (2019) used compound factor method; Rahmati et al., (2019) used the weighted aggregate investigation method; Pham et al., (2018) employed the model of soil disintegration; Tripathi et al., (2003) used the soil and water evaluation model; and Farhan et al., (2018) used the multivariate method.

However, the multi-criteria decision-making methods are mostly preferred methods, such as the analytical hierarchical process (AHP), the fuzzy AHP, the complex corresponding appraisal of choices, the technique for order preference by similarity to an ideal solution and the straightforward added substance weighting. These methods were broadly employed in many studies including (Meshram et al., 2020; Jaiswal et al., 2015; Rahaman et al., 2015; Akay & Baduna Koçyiğit, 2020).

The foremost advantage of GIS-based multi-criteria decision-making method is that it allows evaluating various factors with multi-criteria attributes for watershed prioritization and further utilized for decision makers. The present study used the same concept focusing on the drainage features and the land covers patterns of Teesta River basin and related sub-watersheds evaluated in MCA method considering their role in accelerating the soil erosion (Pal, 2016; Tamang et al., 2012; Wadadar, 2016).

This research will help to understand the soil erosion susceptibility of Middle and Lower Teesta River basin, which can be an aid for decision makers to identify the erosion-prone areas in improving it through scientific or indigenous method of the study area.

2 Study area

Middle and Lower Teesta River basin of Sikkim Himalaya falls in between $88^{\circ}17'5''$ E to $88^{\circ}55'54''$ E longitude and $27^{\circ}4'34''$ N to $27^{\circ}4'36''$ N latitude and covers an area of 2524.59 sq. km. (Fig. 1). Teesta River is a perennial river that is also the trunk river in Sikkim Himalaya. It originates from Tso Lamo lake of Trans Himalayan region; Northern part of Sikkim state flows from north to south and divides the state into two parts. It flows down

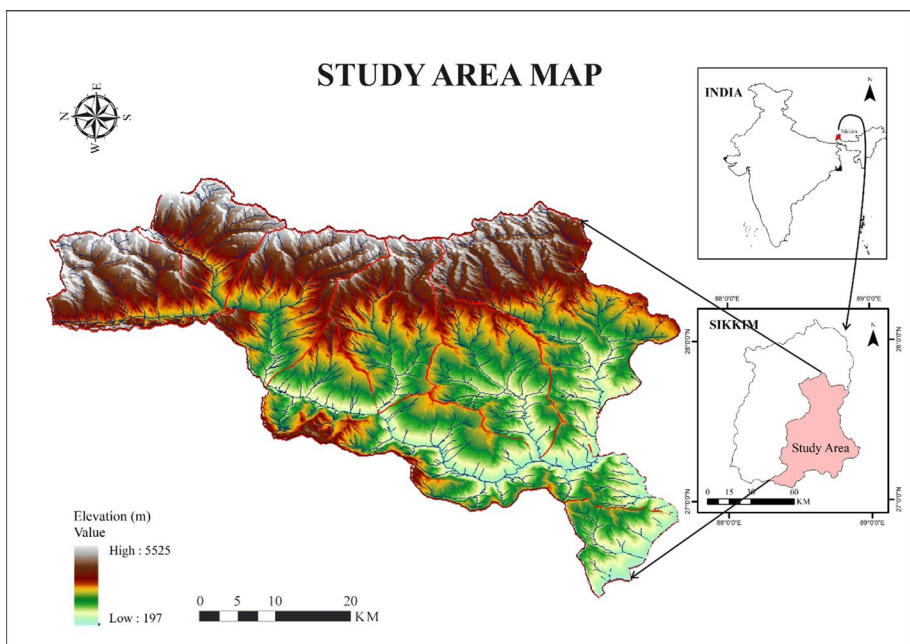


Fig. 1 Study area map of Middle and Lower Teesta basin, Sikkim Himalaya, India

to the parts of North Bengal and Bangladesh, and it finally joins the Bay of Bengal. Topographically, the area lies at the Higher Himalaya, which consists of steep-sided hills and deep valleys.

Lesser Himalaya Sequence (LHS) dominates the study area, which is bordered to the south by Main Boundary Thrust (MBT) and to the north by Main Central Thrust (MCT). The Central Crystalline Gneissic Complex (Proterozoic age), Daling Group (Paleoproterozoic age), Lingtse Granite Gneiss Group (Meso-Proterozoic age) and Gondwana Group (Late Paleozoic age) cover more than 90% of the study area and rest (10%) is unmapped area because of presence of snow cover. These 4 groups make the lithological set up of the study area. The Central Crystalline Gneissic Complex (CCGC), the most abundant rock group found in SW3, SW4, SW5, SW6, SW7 and SW8 of the study area which constituted by calc-silicates, calc-gneisses, quartzites and schists; parts of the CCGC are prone to erosion due to the presence of semi soft nature type of rocks. The Daling Group of rock was exposed in the Teesta valley, the second largest abundant rock group was found in SW1, SW2, SW6 and SW7. The un-fossiliferous low-grade meta-sediments divided into dominantly greenish argillaceous assemblage comprising the Daling “Series” and dolostone, quartzite and variegated slate assemblage making up the Buxa “Series” by Mallet (1875). The Daling Group of rocks are also prone to erosion due to the types of rocks, which are softer in nature. Granite gneiss types of rocks are the main constituent in the Lingtse Granite Gneiss group, found in SW6, SW7 and SW8. The gneisses appear sheet-like bodies of coarse to medium grained, foliated to strongly lineated granite mylonite. The Lower Gondwana rocks, of the LHS, are the Teesta dome’s youngest stratigraphic boundary, which found only in SW2 of the study area. The older Rangit Pebble Slate (RPS), which dates from the early Permian period, is constituted by sandy and pebbly spotted slates of diamictite, fine-grained sandstone and granite, usually easily erodible. (Acharyya and Ray, 1977).

The major type of soil found in Sikkim is the loamy type of soil. According to the strategic and extension plan of East Sikkim, the soils found between 15 and 30% slopes are deep excessively drained, coarse loamy to the fine loamy surface with slight stoniness and moderate erosion. Soils are moderately acidic and rich in humus contain. These areas are also predominantly under forest & cultivation. The soils on ridges of steeply sloppy hill-sides (30–50%) slopes are moderately shallow to deep, well drained, silty to fine loamy soils with slight stoniness and moderate erosion. The soil is acidic and stony surface. They are largely under temperate forest. Alpine forests and some are under cultivation crops. Soils on ridges of more than 50% slope are moderately deep developed on steep sloppy hills, excessively drained, coarse loamy to fine loamy soil with slight stoniness and moderate erosion. Soils are moderately acidic, dark brown to dark yellows and rich in humus. Un-terraced lands are susceptible to severe erosions. These are largely under temperate forest covers.

3 Data set and methodology

3.1 Data set

Numerous data sets have been indulged in achieving the objectives of the given study—(a) ASTER DEM (Advanced Space borne Thermal Emission and Reflection Radiometer) having cell size of 30 m downloaded from (<https://asterweb.jpl.nasa.gov/data.asp>); (b) Sentinel-2A (<https://sentinel.esa.int/web/sentinel/sentinel-data-access>)

of 10 m pixel size considering the bands (2, 3, 4 and 8). To produce details of the land use land cover pertaining to the study area used supervised classification method. Downloaded the watershed map published by Soil and Land Use Survey of India (SLUSI) (<https://slusi.dacnet.nic.in/>) has been used to validate the watershed boundary and drainage network which generated through ASTER DEM. The ancillary data sets such as Geological map from Bhukosh, (<http://bhukosh.gsi.gov.in/Bhukosh/Public>) GSI (Geological Survey of India), are used to understand the geology for the interpretation of soil erosion prone area. During the field survey of the study area, photographs of the erosion-prone areas were taken.

4 Methodology

In the present study, an integrated approach is employed for identification of erosion prone areas in the Middle and Lower Teesta river watershed. The linear-, areal- and relief-based morphometric parameters are generated using ASTER DEM with Spatial Analyst Tools (ArcGIS 10.2). In GIS, environment generated various layers, which are required for morphometric analysis such as slope, aspect, flow accumulation, threshold condition, stream order and basin boundary. As well, an entire watershed was discretized into 8 sub-watersheds and coded as morphometry SW-1 to SW-8. The morphometric parameters are estimated with respect to the delineated sub-watersheds polygon. The sub-watersheds dimension was obtained summing the main channel length and the distance between the higher and lower main channel points to the basin perimeter. Stream order was designated after Strahler hierarchical ranking (Strahler, 1952). Different equations as given in Table 1 developed by many scholars were used in this study to derive the relevant sub-watersheds morphometric parameters corresponding to linear, areal and shape (Abdeta et al., 2020).

Land cover classification (LC), the study employed the multispectral Sentinel-2A data of S2MS12A product type with 10 m spatial resolution acquired on December 16, 2018. The acquired data have already geometrically corrected, processed for layer stacking using bands (2, 3, 4 and 8). The maximum likelihood classification (MLC) was used for the land cover classification processed in ERDAS IMAGINE 14. Numerous image augmentation techniques were engaged in order to achieve heterogeneity taking into consideration the ground truth information with respect to known land cover types of training samples. A total of seven such LC classes were identified for the study area, viz., snow, water body, built-up, barren land, agriculture, dense forest and sparse forest. Field verification (349 ground points) has been finally conducted for the generated LC classes (Fig. 2).

The generated LC map was subjected to the accuracy assessment, using the Kappa coefficient (Altaf et al., 2014). The kappa coefficient indicator used in many studies to check the overall accuracy of the classified image (Foody, 2002). Following is the formula used for calculation of kappa coefficient (Eq. 1.1).

$$k = \frac{\{N \sum_{i=1}^r (X_{ii}) - N \sum_{i=1}^r (X_{i+} \cdot X_{+i})\}}{N^2 - \sum_{i=1}^r (X_{i+} \cdot X_{+i})} \quad (1.1)$$

where k is the kappa coefficient, r rows number included in the error matrix, X_{ii} observations number in row i and column i (on the major diagonal). Whereas the X_{i+} is the total observations in row i (shown a marginal total to right of the matrix), X_{+i} is the total

Table 1 Estimation formulae for morphometric parameters

Estimation of morphometric parameters			
Estimation of linear parameters			
Sl. No	Parameters	Formula/Definition	References
1	Stream order (μ)	Ranking hierarchically	Strahler (1964)
2	Stream length (L_μ)	Total length of the stream segments of that particular order	Horton (1945)
3	Mean stream length (L)	$L = \sum L_\mu / N_\mu$	Strahler (1964)
4	Stream length ratio (R_l)	$R_l = L / L_{(\mu-1)}$ where $L =$ The mean length of all stream segments of a given order (μ) $L_{(\mu-1)} =$ The mean length of all stream segments of one order less to given order (μ)	Horton (1945)
5	Bifurcation ratio (R_b)	$R_b = N_\mu / N_{(\mu+1)}$ where $N_\mu =$ Total number of stream segments of the order " μ ", $N_{(\mu+1)} =$ number of stream segments of the next higher order	Schumm (1956)
6	Drainage density (D_d)	$D_d = \sum L_\mu / A$ where $\sum L_\mu =$ Total length of the stream segments of all orders $A =$ area of the river basin or grid (km^2)	Horton (1932)
7	Texture ratio	Number of stream segments of all order present in per perimeter of that area	Horton (1945)
8	Length of overland flow (L_o)	$L_o = 1/2D_d$ where $D_d =$ drainage density of basin	Horton (1945)
Estimation of areal parameters			
1	Circularity ratio (R_c)	$R_c = 4\pi A / P^2$ where $A =$ area of the basin (km^2), $P =$ perimeter (km)	Miller (1953) Strahler (1964)
2	Elongation ratio (R_e)	$Re = D/L = \frac{1.2\sqrt{A}}{L}$ where $D =$ diameter of a circle of the same area (A) as the basin, $A =$ Area of the basin (km^2), $L =$ basin length (km)	Schumm (1956)
3	Form Factor (F_f)	$F_f = A/L^2$ where $A =$ area of the basin (km^2), $L =$ basin length (km)	Horton (1932, 1945)
4	Compactness constant (C_c)	Ratio between basin perimeters to the perimeter of a circle to the same area	Horton (1945)
5	Drainage texture (T)	$T = D_d \times F_f$ where $D_d =$ drainage density, $F_f =$ stream frequency	Horton (1945)

Table 1 (continued)

Estimation of morphometric parameters		
Estimation of linear parameters		
Sl. No	Parameters	Formula/Definition
6	Shape factor (B_s)	$B_s = L^2/A$ where L = basin length (km), A = area of the Basin (Km^2)
7	Constant of channel maintenance (C)	$C = 1/D_d$ where D_d = drainage density of basin
8	Drainage Frequency (F_μ)	$F_\mu = N_\mu/A$
Estimation of relief aspects		
1	Basin relief (R)	$R = H-h$ where H = maximum elevation (m), h = minimum elevation (m)
2	Relief ratio (R_r)	$R_r = R/L$ where R = basin relief, L = longest axis of the major river (basin length) in km
		References
		Horton (1932)
		Schumm (1956)
		Horton (1932)
		Handley and Schumm (1961)
		Schumm (1956)

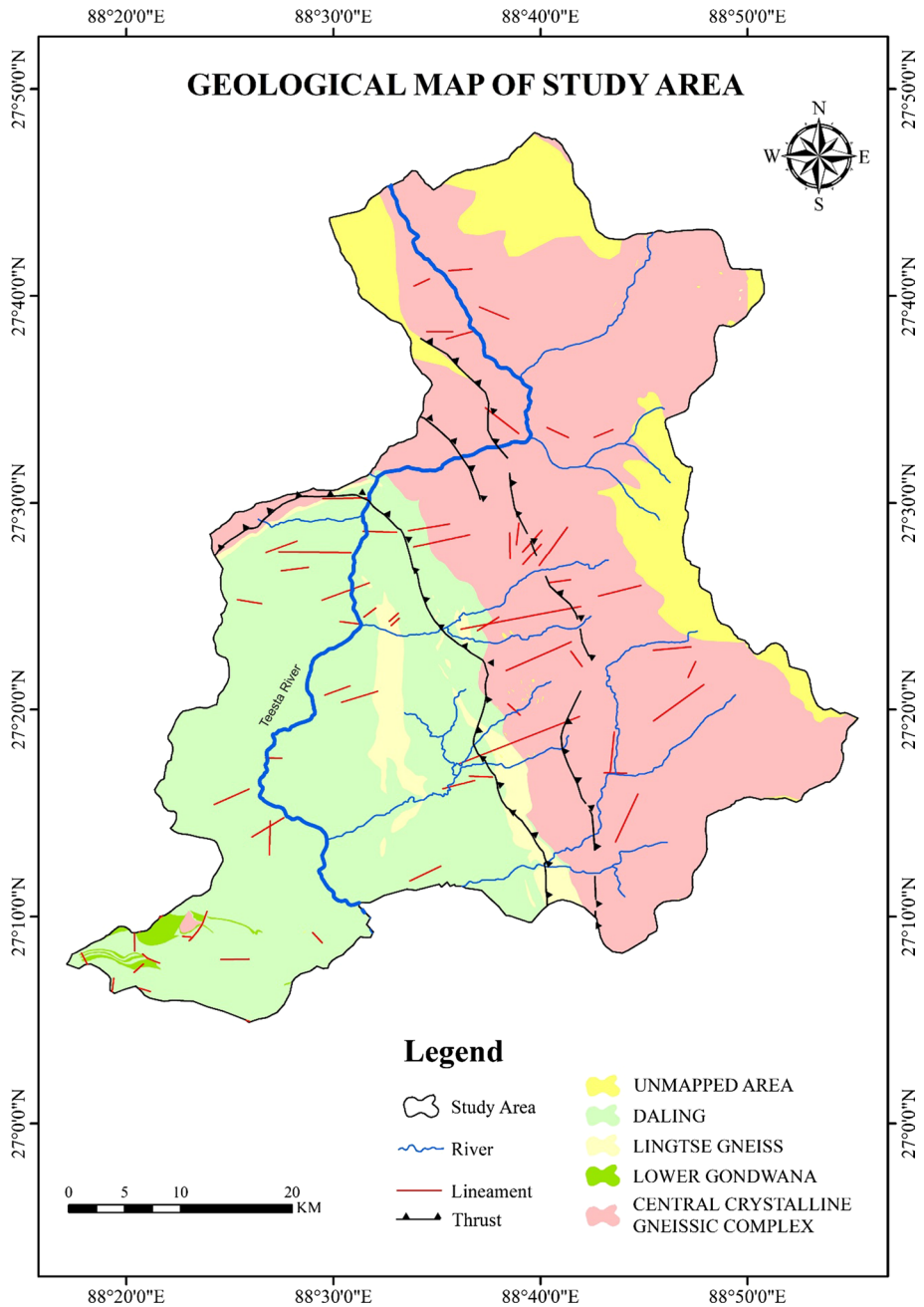


Fig. 2 Geological map of the study area. Source: <https://bhukosh.gsi.gov.in/Bhukosh/MapViewer.aspx>

observations in column i (shown a marginal total at the bottom of the matrix) and N is the total observations number.

The compound value method was used in this study for the multi-criteria analysis. This method transforms a phenomenon from a qualitative aspect into quantitative evaluation (Todorovski & Džeroski, 2006). The MCA method has demonstrated its capability in many studies including (Hembram & Saha, 2020; Trabucchi et al., 2013) for comparison between similar geographic location considering the land surface processes (Mosbahi et al., 2013). In a situation of the data-scarce region, various scholars (Chen et al., 2011; McCloskey et al., 2011; Saghafian et al., 2013) extensively used the methodology for sustainable planning and administration of sub-watersheds. The methodology flowchart is given in Fig. 3.

The entire approach is based on the level of susceptibility of different sub-watersheds to erosion. The process starts by ranking the overall sub-watersheds with respect to both morphometric parameters and land cover. The total number of sub-watersheds are considered to determine the maximum number of rank. In this case, the rank was found in the range between 1 and 8. The lower value 1 was assigned to a morphometric parameter and Lc with respect to their contribution to accelerating the erosion process, while 8 represented the lowest influence on erosion. For a specific sub-watershed, the average rank is calculated and consigned as the compound value (Cp). Henceforth, Cp represents the joint effect of the studied parameters to assess the sub-watersheds erosion vulnerability. Based on the cp value assessed the sub-watershed's susceptibility to erosion. The following formula was used to calculate the compound value (Eq. 1.2).

$$Cp = 1/n \sum_{i=1}^n R \quad (1.2)$$

Here: Cp: compound value; R; parameter's rank; n total parameters number.

5 Results

5.1 Relationship between the morphometric parameters and erosion susceptibility assessment

Watershed morphometric comprises various surface mechanisms including the geology, hydrology and geomorphology (Eniolorunda, 2012). Hence, it becomes a potential indicator of landform structure, hydrogeological processes such as infiltration capacity, soil erodibility and runoff characteristics of a given basin (Sharma et al., 1986). Various studies which used morphometric parameters in soil erosion risk assessment have shown that linear (stream order, stream length, mean stream length, stream length ratio, texture ratio, drainage density, stream frequency, bifurcation ratio, length of overland flow) and relief (Total relief) aspects are directly correlated to the soil erodibility, which means that the severity of soil erosion increases as the values of the aforesaid aspects increase, conversely to areal aspect (circularity ratio, form factor, elongation ratio, compactness coefficient, basin shape, constant of channel maintenance) is inversely correlated to soil erodibility (Nooka et al., 2005).

Toward the assessment of erosion risk in Teesta River basin based on morphometric parameters, the contribution of each morphometric parameters was considered in computation of the average ranks known as compound value (Cp). This Cp calculated, respectively, for each sub-watershed is the summation of ranks over the total number of parameters and accordingly four classes were categorized: very high, high, medium and

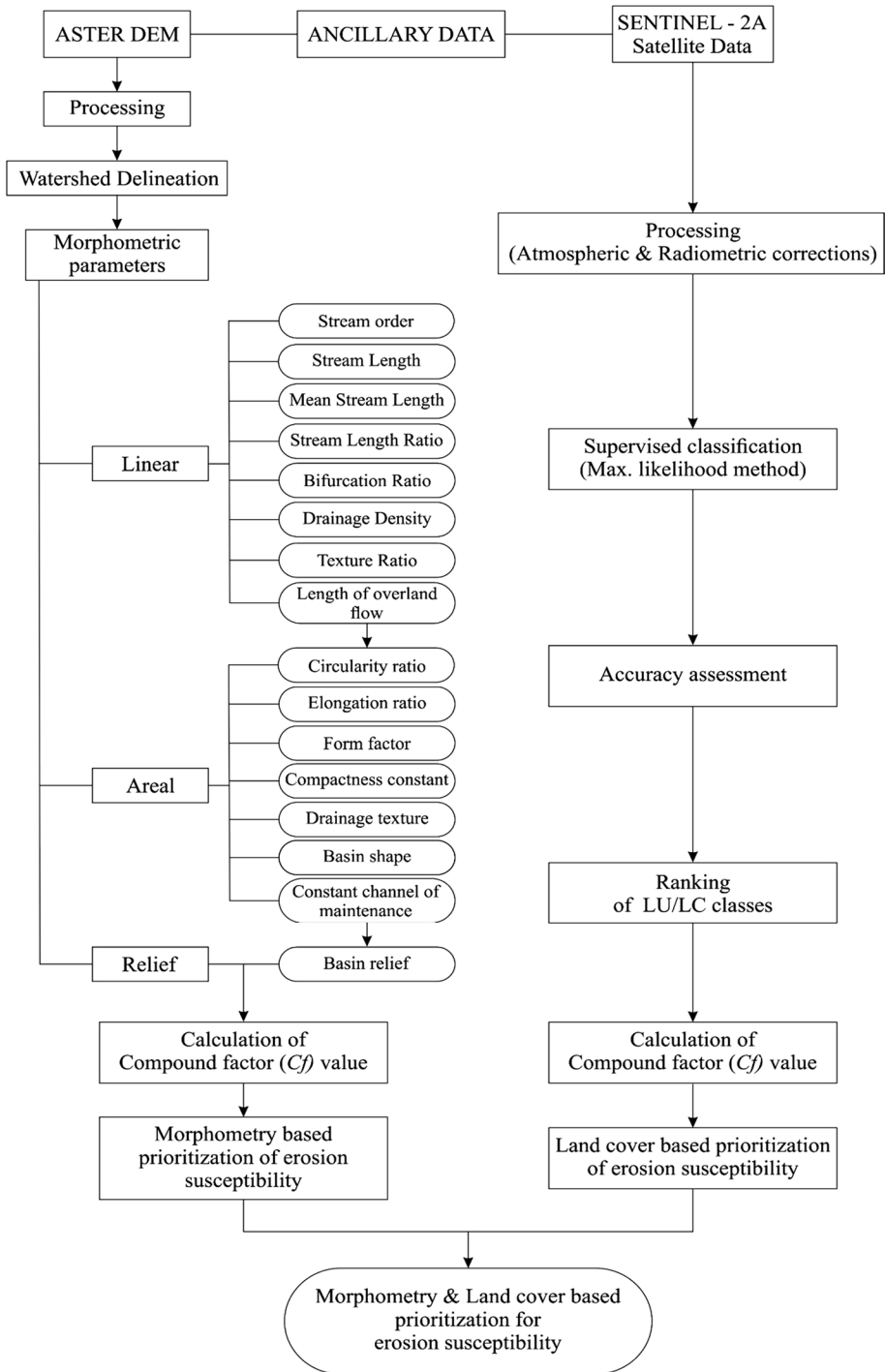


Fig. 3 Flowchart of methodology

low, where the sub-watershed having the lowest compound value is likely to undergo intense erosion (Biswas et al., 1999), hence assigned as very high priority, and next higher value gets high priority and so on until the overall sub-watersheds are ranked.

It has been observed that a dendritic drainage pattern of the entire Middle and Lower Teesta basin is normally observed in many natural rivers. The smallest sub-watershed area was 81.77 km², and largest was 599.86 km². More detail is given in Table 2.

5.2 Linear aspect parameters

In this study, the linear aspects consist of stream order, stream length, mean stream length, stream length ratio, texture ratio, drainage density, stream frequency, bifurcation ratio and length of overland flow.

5.2.1 Stream order

Streams hierarchical position is important to understand any drainage characteristics of a given basin. This parameter was calculated based on stream order model proposed by Strahler (1957). Teesta River basin is classified as 6th order basin. Table 2 and Fig. 4 that give more detail about the sub-watersheds area, stream order and total number of streams per order and per sub-watershed revealed that Teesta River basin had total streams number of 838 (highest streams number 186 found in SW-8 while lowest streams number found in SW-2), out of which 75.63% (633) is 1st order, (18.52%) is 2nd order, 4.42% (37) is 3rd order, 0.95% (8) is 4th order, 0.48% (4) is 5th order, and 0.12% (1) is 6th order.

It has been observed that the number of streams decreased as the stream order increased, which means that the frequency of streams decreased in increasing stream order. The basin of such a type indicates the direction of flow from high altitude to low altitude.

Table 2 Sub-watershed wise stream order with number of segments

Sl. No	Sub-watershed	Area (km ²)	Number of streams						Total
			I	II	III	IV	V	VI	
1	SW1	599.86	82	34	8		1	1	126
2	SW2	81.77	22	5	1				28
3	SW3	270.95	72	18	5	1	1		97
4	SW4	294.04	96	19	4	1			120
5	SW5	200.47	53	12	3	1			69
6	SW6	245.95	85	17	6	2	1		111
7	SW7	252.27	77	19	4	1			101
8	SW8	508.73	146	31	6	2	1		186
Total		2454.03	633	155	37	8	4	1	838
Percentage (%)			75.63	18.52	4.42	0.95	0.48	0.12	100

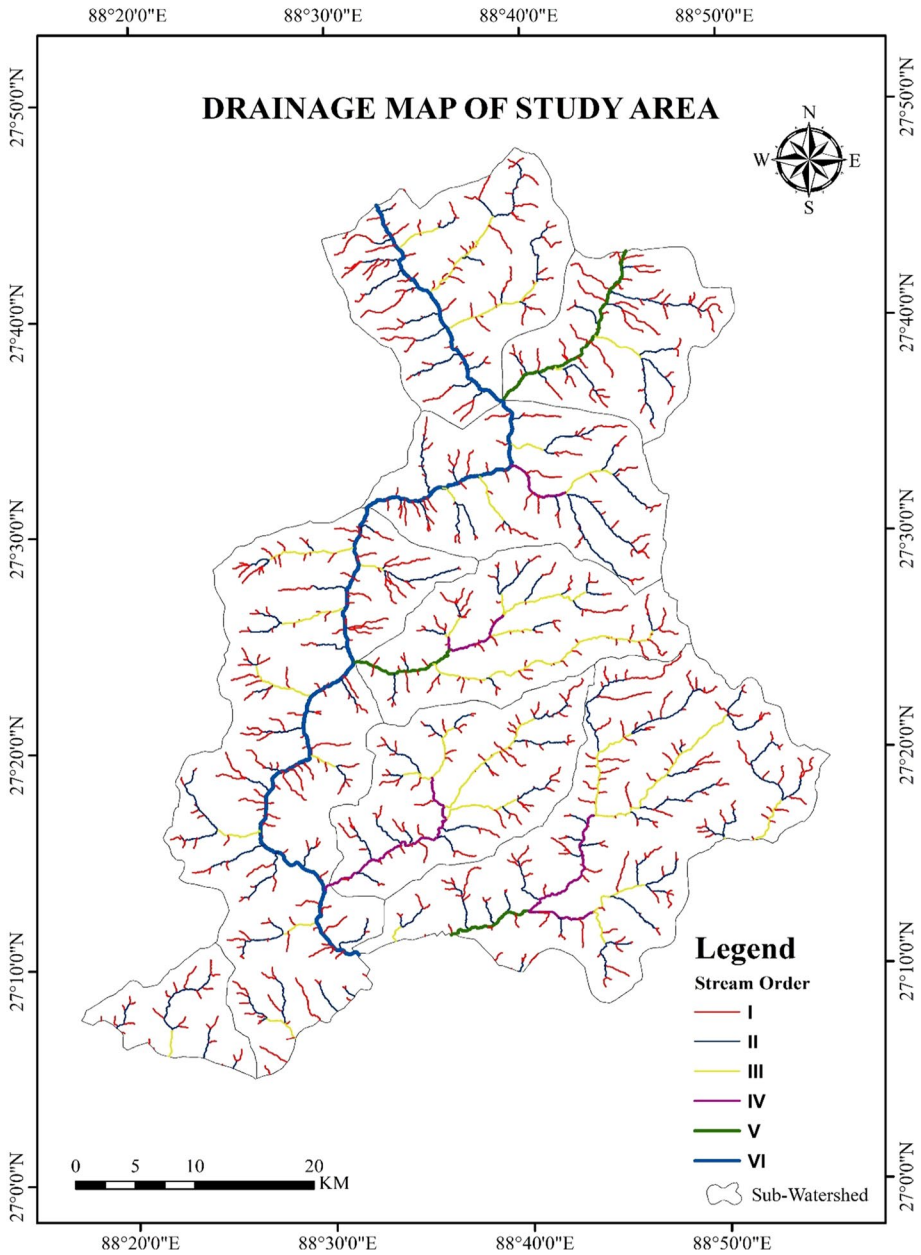


Fig. 4 Drainage map of the study area

5.2.2 Stream length

This parameter was calculated after Horton's second law (Horton, 1945) that goes, the total length of streams decreases as the stream order increases, which means that the highest total stream length would be always found in the lowest stream order. The results

Table 3 Sub-watershed wise stream order with stream length

Sl. No	Sub-watershed	Area	Stream length in Km						Total
			I	II	III	IV	V	VI	
1	SW1	599.86	202.92	88.71	37.83		18.71	36.27	384.44
2	SW2	81.77	21.09	11.92	2.53				35.54
3	SW3	270.95	77.66	53.97	15.56	11.65	21.77		180.61
4	SW4	294.04	100.44	52.92	24.50	21.06			198.92
5	SW5	200.47	79.47	31.15	12.82	11.05			134.49
6	SW6	245.95	67.35	27.35	40.86	7.63	9.77		152.96
7	SW7	252.27	71.02	41.83	28.57	19.47			160.89
8	SW8	508.73	157.74	102.09	42.83	18.94	7.94		329.54
Total		2454.03	777.69	409.94	205.50	89.80	58.19	36.27	1577.39
Percentage (%)			49.30	25.99	13.03	5.69	3.69	2.30	100.00

Table 4 Sub-watershed wise stream order with mean stream length

Sl. No	Sub-watersheds	Stream length in Km					
		I	II	III	IV	V	VI
1	SW1	2.475	2.609	4.729		18.710	36.270
2	SW2	0.959	2.384	2.530			
3	SW3	1.079	2.998	3.112	11.650	21.770	
4	SW4	1.046	2.785	6.125	21.060		
5	SW5	1.499	2.596	4.273	11.050		
6	SW6	0.792	1.609	6.810	3.815	9.770	
7	SW7	0.922	2.202	7.143	19.470		
8	SW8	1.080	3.293	7.138	9.470	7.940	
Mean stream length		1.232	2.560	5.232	12.753	14.548	36.270

describing the stream order and associated stream length given in (Table 3 and Fig. 4) show that Teesta River basin follows Horton's law. Out of the total stream length of 1577.39 km (highest total streams length in SW-1 and lowest total length of streams in SW-2), the highest total stream length 777.69Km was found in 1st order, 409.94 km is 2nd order, 205. Km in 3rd order, 89.8 km in 4th order, 58.19 km in the order, and the lowest total stream length was found in 6th order.

This change might be due to the variation in slope steepness, variation in lithology and the high altitude to the low altitude flow direction.

5.2.3 Mean stream length

Related to the basin size and basin topography, the mean stream length increases as the stream order also increases which makes this parameter opposite to the Horton law. Table 4 shows that the lowest mean stream length of 1.232 km was observed in 1st order, 2.56 km in 2nd order, 5.232 km in 3rd order, 12.73 km in 4th order, 14.548 km in 5th order and the

highest mean stream length was observed in 6th order. This result can indicate the highest mean annual runoff in 6th stream order as the mean annual rainfall runoff relatively increased as the stream order increased.

5.2.4 Stream length ratio

It is defined as a fraction between the mean stream lengths of one order to that of the next lower order. The stream length ratio for Teesta River basin was found in the range from 0.532 noticed in the first order to 1.939 observed in fifth stream orders which thereby suggest that the geomorphic development is at the late youth stage (Vittala et al., 2004). The result given in (Table 5) revealed that no trends exist between streams of different orders within different sub-watersheds, which might be attributed to the discrepancy existing in slope and topography.

5.2.5 Texture ratio (T)

The texture ratio is the ratio between the first streams order and the basin perimeter (Horton, 1945). It depends on rainfall, rock type, relief, infiltration capacity and lithology. Smith (1950) proposed four texture classes: coarse texture (<4/km), intermediate texture (4–10/km), fine texture (10–15/km) and ultrafine texture (>15/km). From this classification, it is noticeable that Teesta River basin is categorized as coarse texture <4/km, since drainage texture values of the sub-watersheds vary from 0.618 in SW-2 ranked 8 to 1.63 in SW-4 ranked 1 indicating maximum erosion exposure of the sub-watershed.

5.2.6 Drainage density (D_d)

Drainage density depends on soil properties, vegetation and the dominated climate among others. Drainage density indicates the closeness of channel spacing, runoff, erosion potential and landscape dissection (Yadav et al., 2014). Drainage density values given in Table 6 and Fig. 5 show that Teesta River basin is a well-drained basin $D_d < 1 \text{ km/Km}^2$. The drainage density ranging from 0.43 to 0.68 km/Km^2 in SW-2 ranked 8 and SW-4 ranked 1,

Table 5 Stream length ratio of sub-watershed

Sl. No	Sub-watershed	Stream length ratio					Average
		III/I	III/II	IV/III	V/IV	VI/V	
1	SW1	0.437	0.426			1.939	0.432
2	SW2	0.565	0.212				0.389
3	SW3	0.695	0.288	0.749	1.869		0.900
4	SW4	0.527	0.463	0.860	0.000		0.462
5	SW5	0.392	0.412	0.862	0.000		0.416
6	SW6	0.406	1.494	0.187	1.280		0.842
7	SW7	0.589	0.683	0.681	0.000		0.488
8	SW8	0.647	0.420	0.442	0.419		0.482
Average		0.532	0.550	0.630	0.595	1.939	0.551

Table 6 Morphometry-based watershed prioritization for erosion susceptibility of study area

Sub-watershed	Linear parameters										Shape (areal parameters)						Relief	Cp value	Erosion susceptibility						
	D _d		F _u		R _b		L _o		T		R _c		R _f		R _e					C _c		B _s		C	
SW1	0.64	0.21	3.3	0.32	0.85	0.35	0.24	0.56	1.70	4.11	3.3	3510	8.125	Low priority											
Rank	6	8	7	4	7	1	1	1	8	8	7	7													
SW2	0.43	0.34	4.7	0.22	0.62	0.50	0.32	0.64	1.41	3.13	4.7	2008	8.375	Low priority											
Rank	8	7	1	8	8	3	8	8	6	1	1	8													
SW3	0.67	0.36	3.4	0.33	1.31	0.62	0.27	0.59	1.27	3.69	3.4	4495	7	Medium priority											
Rank	3	5	6	3	5	6	6	6	3	5	6	2													
SW4	0.68	0.41	4.6	0.34	1.63	0.68	0.27	0.58	1.21	3.73	4.6	3973	4.625	Very high priority											
Rank	1	2	2	2	1	8	5	3	1	6	2	4													
SW5	0.67	0.34	3.8	0.34	1.10	0.64	0.28	0.60	1.25	3.54	3.8	3907	6.625	High priority											
Rank	2	6	4	1	6	7	7	7	2	2	4	5													
SW6	0.62	0.45	3.21	0.31	1.49	0.55	0.27	0.59	1.34	3.64	3.21	4558	6.875	Medium priority											
Rank	7	1	8	7	2	4	4	5	5	3	8	1													
SW7	0.64	0.4	4.27	0.32	1.35	0.57	0.27	0.59	1.33	3.65	4.27	3731	6.125	Very high priority											
Rank	5	3	3	5	4	5	3	4	4	4	3	6													
SW8	0.65	0.37	3.72	0.32	1.48	0.40	0.25	0.56	1.57	4.02	3.72	4395	6.25	High priority											
Rank	4	4	5	6	3	2	2	2	7	7	5	3													

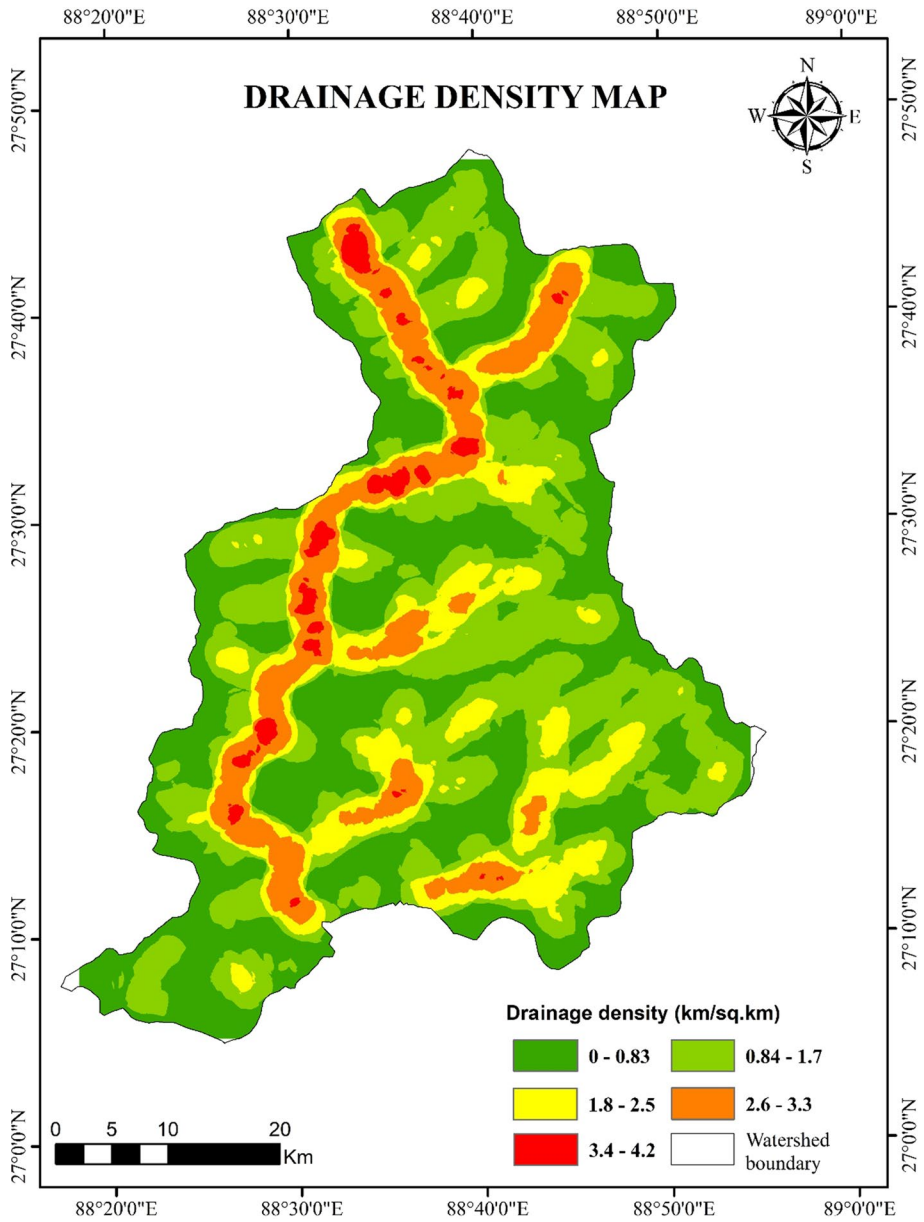


Fig. 5 Drainage density map of the study area

respectively, denotes low density of the sub-watersheds. Therefore, it indicates high to low soil permeability, low to high relief and low to high susceptibility to erosion.

5.2.7 Stream frequency (F_u)

Stream frequency is closely related to basin relief but inversely related to subsoil permeability and infiltration capacity of a terrain (Montgomery and Dietrich, 1992). The high stream frequency value related to marginal topography thus high rainfall runoff of the terrain. This means, the lower the relief and the more water infiltrates, the lower the stream frequency and the higher the slope result to higher runoff led to high susceptibility to soil erosion.

The values of stream frequency given in Table 6 notice the maximum susceptibility in SW-6 ($0.45/\text{km}^2$) and minimum proneness to erosion in SW-1 ($0.21/\text{km}^2$), thus ranked 1 and 8.

5.2.8 Bifurcation ratio (R_b)

It is the only morphometric parameter to be associated with lithological and geological development in the drainage pattern Schumm (1956). R_b values tabulated in Table 6; the bifurcation ratio for the Teesta River basin ranging from 3.21 to 4.7 resulted in the average of 3.879 that indicates well-developed and undistorted natural drainage system (Strahler, 1964), where low R_b values are found on plain terrain or might be caused by greater numbers of 1st and 2nd streams orders (Kumar et al., 2011). The analysis revealed that lowest R_b value was recorded in SW-6 ranked 8, denoting good subsoil permeability thus low runoff contrary to SW-2 ranked 1, recorded the highest R_b values signifying low subsoil permeability thus maximum susceptibility to soil erosion (Bhattacharya et al., 2019).

5.2.9 Length of overland flow (L_o)

According to Horton (1945), L_o represents the length of water flowing over the surface before it gets concentrated into a specific drainage network. Hence, according to Horton (1932) L_o independently affects the physiographic and hydrologic development of the basin drainage. L_o is lower in steeper slopes while higher for gentle slopes. Consequently, it has a direct relation with channel slope. As shown in Table 6, the length of overland flow varies from 0.22 km to 0.34 km. If the L_g value is between 0.2 and 0.3 km indicating the presence of moderate ground slope, moderate infiltration associated with moderate runoff. SW-5 ranked 1 has the highest L_o value indicating potential erosion because the rainfall might take a long duration to reach a given drainage network, thus increasing the susceptibility to erosion in opposite to SW-2 recorded lowest L_o value denoting moderate infiltration and low runoff.

5.3 Shape/Areal parameters

Areal aspects consist of circularity ratio, elongation ratio, form factor, compactness coefficient, basin shape and constant of channel maintenance.

5.3.1 Circularity ratio (R_c)

Circular ratio is one of the most important areal parameters defined by Miller (1953) as the ratio of basin area to the area of a circle having the same circumference as the basin. Typically circular shapes have higher R_c and indicate permeable subsoil surface and moderate

to high relief, whereas elongated shape has low R_c suggests impermeable surface and low relief. For different sub-watersheds, R_c values vary from 0.35 to 0.68 (Table 6). SW-1 ranked 1 recorded the low R_c value, while SW-4 recorded highest R_c value, hence ranked 8.

5.3.2 Form Factor (R_f)

According to Horton (1932), this dimensionless areal parameter represents the ratio of basin area to the square of basin length. A perfectly circular basin the form factor value is less than 0.7854, while a form factor greater than 0.8 indicates high peak flow of short duration. Given in Table 6, the analysis of form factor revealed a variation from 0.24 to 0.32 which indicates elongated shape for sub-watersheds with lower peak flow of longer duration. The most susceptible sub-watershed was SW-1 while the least erosion prone was SW-2 having low to high form factor values, respectively.

5.3.3 Elongation ratio (R_e)

Elongation ratio depends on climate and geological development of a terrain (Rudraiah et al., 2008). Elongation is always categorized in 4 classes: 0.9–1.0 (circular), 0.8–0.9 (oval), 0.7–0.8 (less elongated), 0.5–0.7 (elongated) and <0.5 (more elongated). Low relief obviously has R_e approaching 1.0, while R_e values that range from 0.6 to 0.8 are commonly found in steep slope area (Dar et al. 2013). R_e values given in Table 6 show that Teesta River basin is elongated in shape thus associated with steep slope and high relief since R_e values of sub-watersheds were found between 0.5 and 0.7. In the study area, the R_e variation was 0.58 in SW-1 and 8 to 0.64 in SW-2 thus ranked 1 and 8, respectively.

5.3.4 Compactness coefficient (C_c)

A basin is more elongated if the C_c values are lower, while a basin is circular if C_c values are higher. C_c for Teesta River basin varies from 1.21 to 1.70. This means that sub-watersheds are elongated in shape, i.e., poor discharge capacity. SW-4 recorded the lowest C_c value thus ranked 1, and SW-1 recorded the highest C_c value, hence ranked 8.

5.3.5 Basin shape (B_s)

Basin shape is analyzed using basin length and basin area. Result given in Table 6 revealed that, in sub-watersheds, basin shape values range from 3.13 to 4.11 denoting elongated shape of the sub-watersheds. Consequently, the basin inefficiently discharges the amount of runoff which is easier in a circular basin. The lower the B_s values, the more erosion and vice versa. Therefore, SW-2 (Ranked 1) is the most susceptible as compared to SW-1 (Rank 8) which is less susceptible to erosion.

5.3.6 Constant of channel maintenance (C)

Throughout the eight sub-watersheds of Teesta River basin, the constant of channel maintenance range from 3.21 to 4.7. Lower C values for SW-6 denote less structure control on weak structure control on low permeable surface compared to the SW-2 having higher C values that indicates more structure control on high permeable surface.

5.4 Relief parameter

5.4.1 Basin relief/total relief (H)

Total relief (H) is simply the difference in elevation between maximum and the minimum points of a basin. H has a strong correlation with hydrological characters of a basin (Schumm, 1956). In addition, H indicates the steepness, which increases the erosion intensity in a drainage basin and the geomorphic activities throughout the basin. In sub-watersheds, basin relief values range from 2008 to 4558 m. Basin relief determine the erosion potential or erosion susceptibility in the drainage network. For instance, the low H value recorded in SW-2 ranked 8 denotes low erosion potential as compared to the high H value observed in SW-6 showing high susceptibility to soil erosion thus ranked 1.

6 Discussion

6.1 Sub-watersheds prioritization based on morphometric parameters

Table 6 and Fig. 6 give the information about erosion susceptibility of sub-watersheds based on morphometry. The results revealed that with respect to morphometric parameters, SW-4 and SW-7 with C_p values 4.62 and 6.12, respectively, fall in “very high priority” sub-watersheds; while SW-5 and SW-8 that have C_p values 6.25 and 6.62, respectively, belong to “high priority” category; SW-6 and SW-3 with C_p values of 6.87 and 7 appertained to “medium priority” group; and finally SW-1 and SW-2 that have C_p values of 8.12 and 8.37, respectively, belong to the “low priority” category.

The sub-watersheds SW4, SW7, SW8 and SW5 are critical sub-watersheds, which contribute largest amount of soil in the entire watershed. The main reason behind this is these sub-watersheds have highest slope. Slope determines the erosional as well as geomorphic process. The slopes of these sub-watersheds are more unstable hence; its susceptibility to erosion is more. The SW3 and SW6 fall in medium priority because of moderate slope less drainage density. The SW1 and SW2 falls under low priority to susceptibility of the erosion because of less degree of slope compared to other sub-watersheds.

6.2 Sub-watersheds prioritization based on land cover parameters

Seven major land cover classes were generated for the study area such as water body, dense forest, sparse forest, snow, barren land, agriculture and built-up area (Fig. 7). In this study, identification of land cover types was based on the strong contribution of land cover in accelerating land degradation in form of erosion. The ground verification exercise (post-classification) was undertaken, from which 349 ground truth samples were collected.

The maximum likelihood classification (MLC) generated an overall accuracy of 95.98% (Table 7), with a Kappa coefficient of 0.98. This accuracy falls in the acceptable; range > 80%, suggested for erosion risk assessment using land covers classes (Foody, 2002). Based on the potential effect of a specific land cover type to trigger erosion, the ranks were assigned to a particular land cover category. Then after, for the prioritization of each sub-watershed, compound values were assessed considering LC category ranking. The lowest priority is given to the larger snow land, cultivation area, more vegetative cover and larger built-up, while the highest priority was given to smaller snow land, cultivation

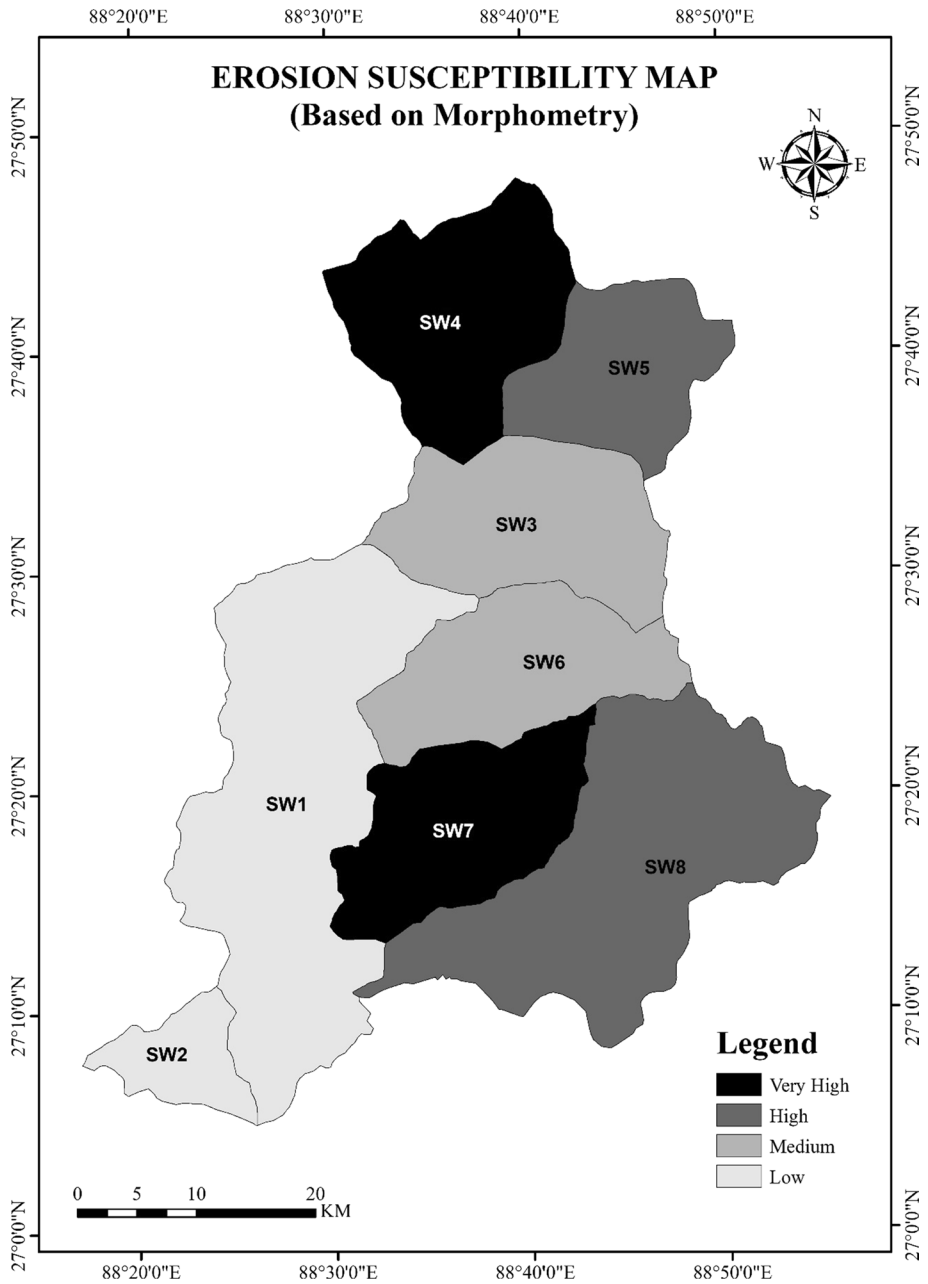


Fig. 6 Morphometry-based watershed prioritization map of the study area

area, lesser vegetative cover and larger barren land. The summarized sub-watersheds LC statistics, Cp values and prioritization are shown in (Table 8).

It has been found that water body that comprises perennial rivers, streams, lakes and pond covered 40.03 Km² (1.63%), dense forest the predominant land cover category with

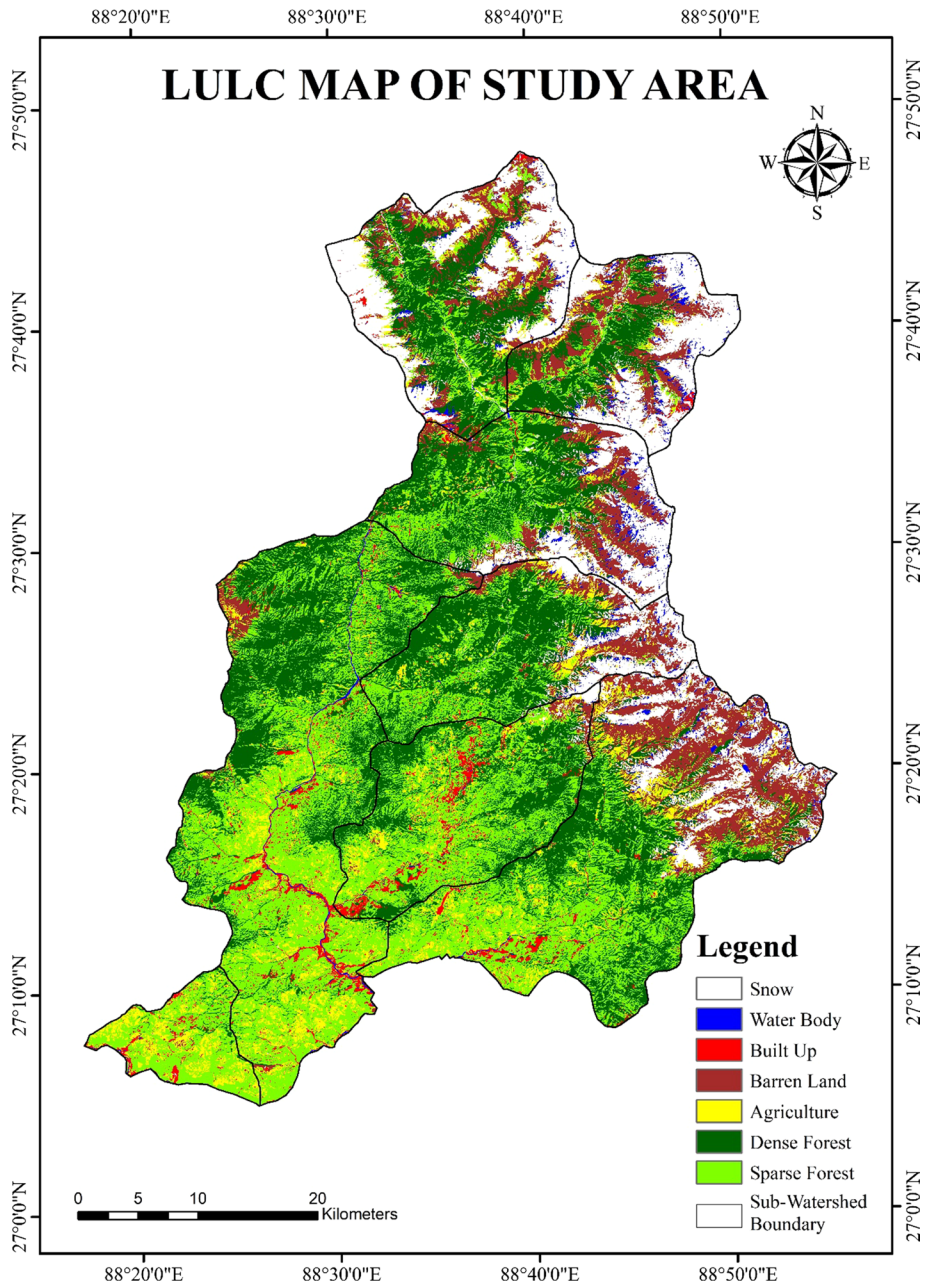


Fig. 7 Land use land cover classification map of study area

40% density of tree canopy occupied 77.8.63 km² (31.73%), sparse forest such as shrubs, agroforestry area and land with tree canopy density between 10 and 40% covered 764.45 km² (31.15%), snow covered 331.38 km² (13.5%), barren land that comprises sediments,

Table 7 Accuracy assessment of land use land cover classification

Reference data									
	DF	S	W	B	Ag	SF	BL	Ground truth total	User's accuracy
<i>Classification data</i>									
DF	45				2		2	49	98
SW		50						50	100
W	1		50					51	98.03
B				45		2	2	49	100
Ag					50			50	100
SF						46	4	50	100
BL							49	50	98
<i>Column Total</i>	46	50	50	46	52	48	57	349	
<i>Producer's Accuracy</i>	90	100	100	90	100	192	98		
Overall accuracy [(45 + 50 + 50 + 45 + 50 + 46 + 49)/349] × 100 = 95.98%									

DF Dense forest, S snow, W water body, B built-up, Ag agriculture, SF sparse forest, BL barren land

exposed rocks, landslides zones and degraded forest area covered 296.2 km² (12.08%), agriculture land occupied 181.22 km² (7.38%), and built-up area shared 62.11 km² (2.53%).

The analysis of compound values as illustrated in (Table 8) revealed that the sub-watersheds SW-3, SW-4 and SW-5 that have Cp values of 3.83, 4 and 4, respectively, were given “very high priority” rank, SW-8 and SW-6 that have Cp values of 4.33 and 4.5, respectively, were ranked as “high priority” sub-watersheds, SW-1 and SW-7 that have Cp values of 5.33 and 5.5, respectively, were assigned “medium priority” rank, and “low priority” was assigned to SW-2 having Cp value of 5.83 (Fig. 8).

7 Assessment of level of susceptibility to erosion based on the combination of land cover and morphometric

Finally, the sub-watersheds were evaluated and prioritized into a multi-criteria analysis based on individual ranking of each morphometric and land cover parameters. Therefore, eight major classes have been classified such as 1, 2, 3, 4, 5, 6, 7 and 8.

The results presented in Table 9 and Fig. 9 indicate that SW4 and SW5 having the first and second lowest Cp values (3.39 and 4) were found to be the most susceptible to erosion, consequently were ranked 1 and 2 indicating the highest prioritized sub-watersheds. The SW-8 and SW-3 were the third and fourth vulnerable sub-watersheds with Cp values of (4.22 and 4.39) ranked 3 and 4, respectively. The SW-6 and SW-7 have the same Cp values of (4.56) rated 5 and 6 denoting “medium priority.” The SW-2 and SW-1 that have Cp values of (5.39 and 5.67) ranked 8 and 7 could be the least prioritized sub-watersheds. Figure 10 shows the actual soil erosion field photographs. The a and b photographs cover the Lower Teesta basin and c, d, e and f which covers middle Teesta basin. Through these photographs, easily the problem of soil severity can be understood. The soil erosion susceptibility map of the Middle and Lower Teesta watershed based on combined effect of morphometry and land cover will be a guideline for making policies at State and National level regarding reducing soil erosion.

Table 8 Land cover area statistics of the study area

Sub-watershed	Snow	Built-up	Barren land	Agriculture	Dense forest	Sparse forest	C_p Value	Erosion susceptibility
SW-1	0.00	4.47	1.94	8.21	33.81	50.29	5.33	Medium
Rank	1	6	7	6	5	7		
SW-2	0.00	5.98	1.20	25.87	4.40	62.25	5.83	Low
Rank	2	8	8	8	1	8		
SW-3	20.63	0.73	17.43	3.35	37.81	17.19	3.83	Very high
Rank	6	3	3	1	7	3		
SW-4	34.61	0.74	16.88	4.73	30.57	10.53	4	Very high
Rank	7	4	4	3	4	2		
SW-5	36.60	0.49	23.58	4.00	24.52	7.03	4	Very high
Rank	8	2	1	2	2	1		
SW-6	14.86	0.40	11.53	5.36	45.22	20.92	4.5	High
Rank	5	1	5	4	8	4		
SW-7	0.67	5.92	2.26	7.46	36.10	46.40	5.5	Medium
Rank	3	7	6	5	6	6		
SW-8	12.21	1.83	20.71	8.69	25.25	29.83	4.33	High
Rank	4	5	2	7	3	5		

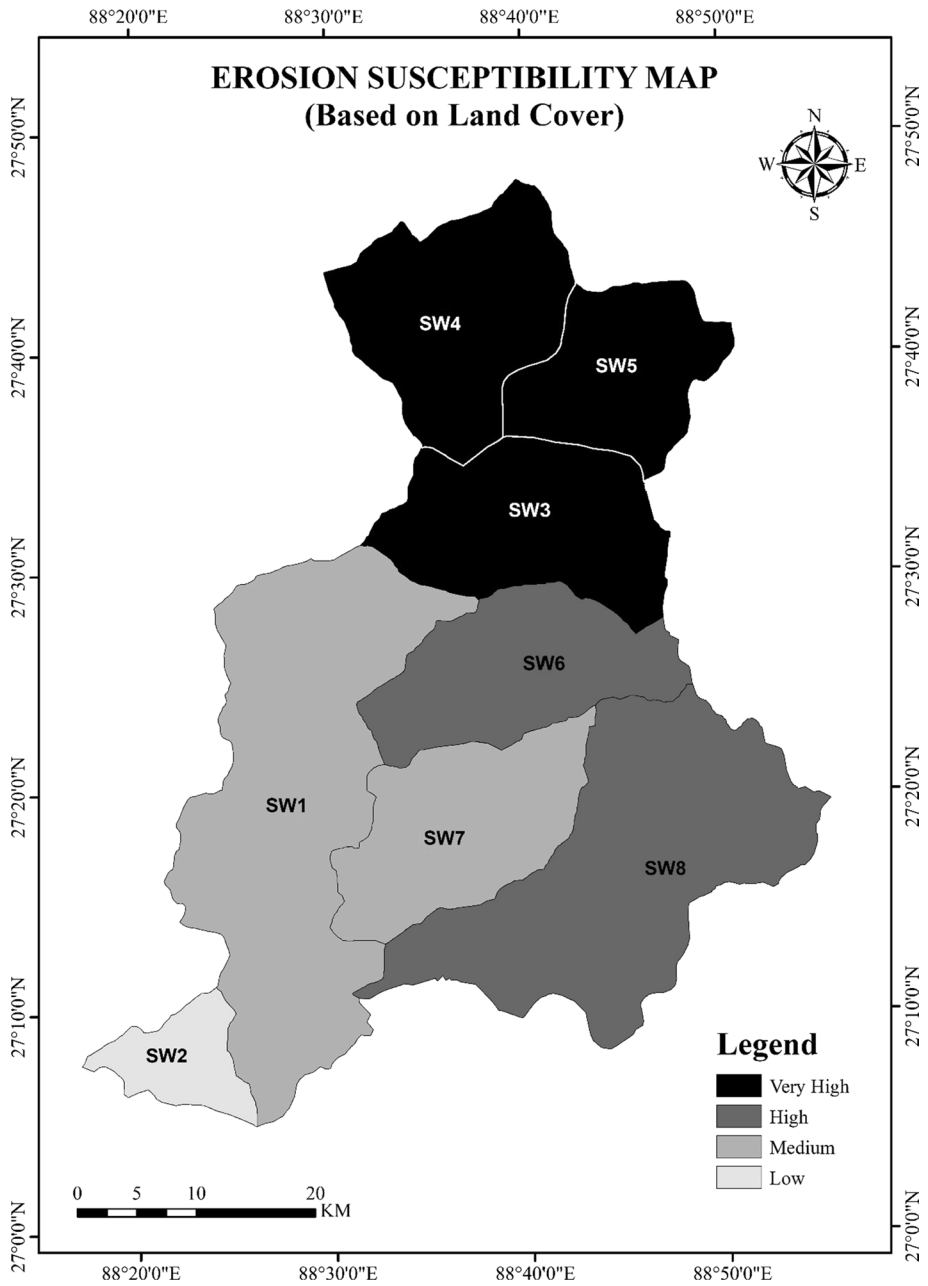


Fig. 8 Land cover-based watershed prioritization map of study area

Table 9 Watershed prioritization for erosion susceptibility of study area based on the combined influences of morphometry and land cover

SW	Morphometric parameters														Cp Value	Erosion Susceptibility				
	Land cover																			
	Relief																			
	Shape (areal parameters)							Land cover												
D _d	F _u	R _b	L _o	T	R _c	R _f	R _e	C _c	B _s	C	H	S	B	BL	Ag	DF	SF			
SW1	6	8	7	4	7	1	1	1	8	8	7	7	1	6	7	6	5	7	5.39	7
SW2	8	7	1	8	8	3	8	8	6	1	1	8	2	8	8	8	1	8	5.67	8
SW3	3	5	6	3	5	6	6	6	3	5	6	2	6	3	3	1	7	3	4.39	4
SW4	1	2	2	2	1	8	5	3	1	6	2	4	7	4	4	3	4	2	3.39	1
SW5	2	6	4	1	6	7	7	7	2	2	4	5	8	2	1	2	2	1	4	2
SW6	7	1	8	7	2	4	4	5	5	3	8	1	5	1	5	4	8	4	4.56	5
SW7	5	3	3	5	4	5	3	4	4	4	3	6	3	7	6	5	6	6	4.56	6
SW8	4	4	5	6	3	2	2	2	7	7	5	3	4	5	2	7	3	5	4.22	3

SW Sub-watershed, D_d drainage density, F_u stream frequency, L_o length of overland flow, T drainage texture, R_c circularity ratio, R_f form factor, R_e elongation ratio, C_c compactness coefficient, B_s basin shape, C constant of channel maintenance, H basin relief, DF dense forest, S snow, W water body, B built-up, Ag agriculture, SF sparse forest, BL barren land

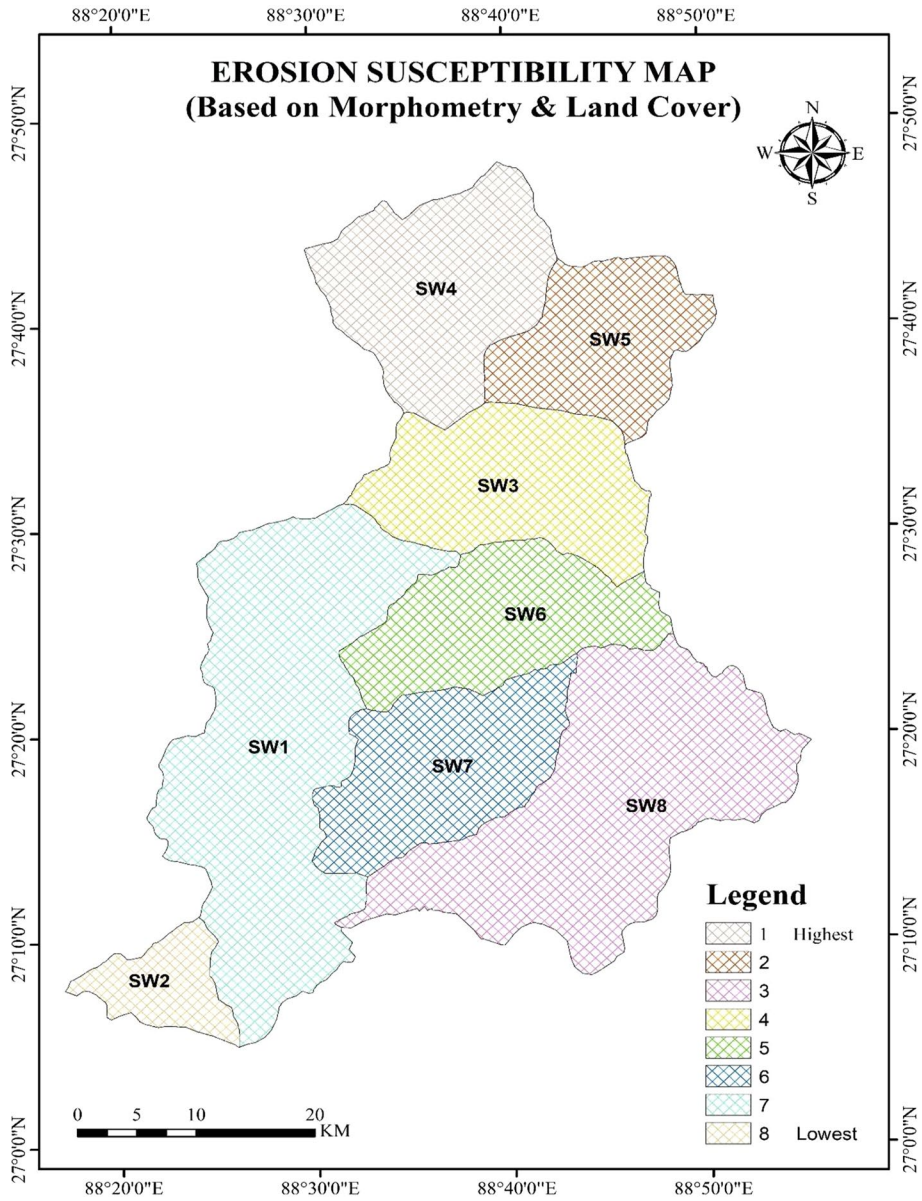


Fig. 9 Watershed prioritization ranking map of study area based on the combined impact of morphometry and land cover

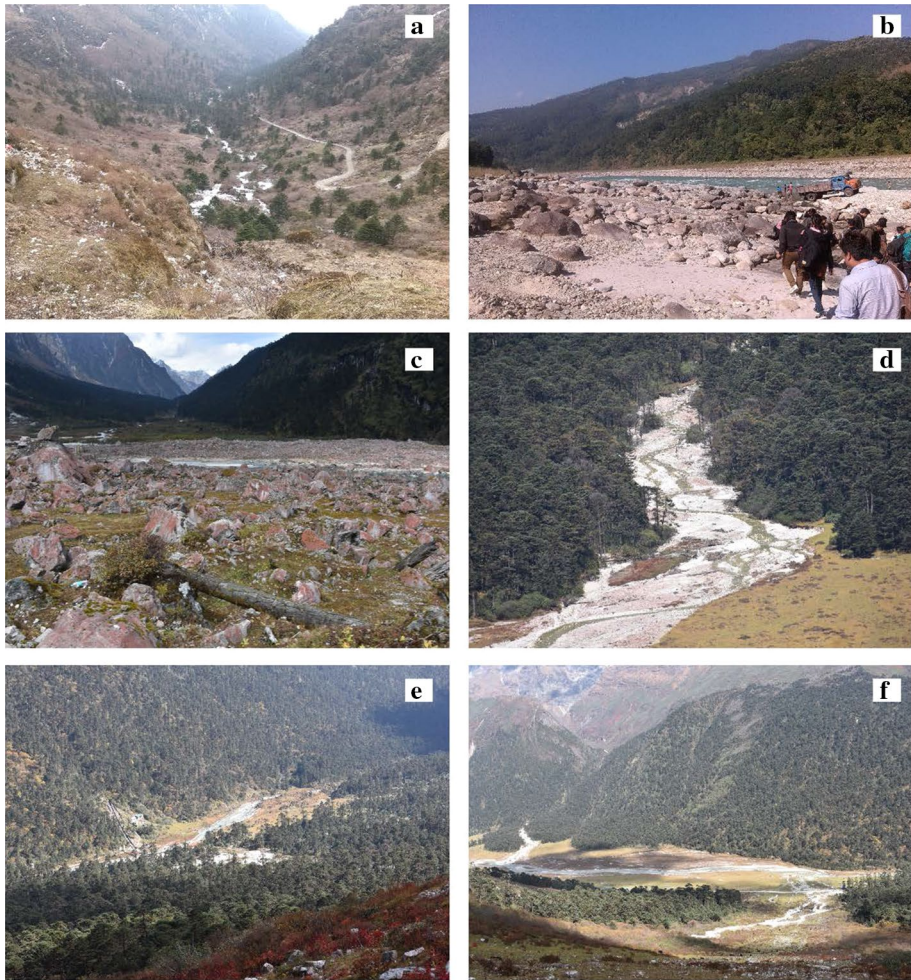


Fig. 10 Field photographs

8 Conclusion

The present study demonstrated the usefulness of Geo-informatics based on multi-criteria method integrated drainage characteristics and land cover categories for identification of risk potential areas. Integration of the morphometric parameters and land cover categories complemented by field verification rather than using conventional method is important to understand hydrogeological behavior of a drainage basin and measure explicitly the level of susceptibility of erosion of sub-watersheds, and hence indicate erosion hotspot areas that are indispensable for the adoption and development of the finest practices of management or indigenous technical system for the sustainable development of land and water resources. The result that come from this study shows that Teesta River basin is a sixth-order river, dendritic drainage type, it is dominated by high relief and slope, elongated in shape indicating lower peak flow of longer duration, it is well developed and undistorted

natural system with the mean bifurcation ratio of 3.879, and dense forest and sparse forest are the most predominant land covers shared 31.73% and 31.1%, respectively. Efforts should be made in sub-watersheds 4 and 5 considered as the most prioritized sub-watersheds followed by SW-8 and 3. While SW-6 and 7 need medium priority, SW-1 and 2 could be given the least priority for mitigation. Therefore, the outcomes are served as an instrument to ensure sustainable use of natural resources.

Declarations

Conflict of interest No potential conflict of interest reported by authors.

References

- Abdeta, G. S., Tesemma, A. B., Tura, A. L., & Atlabachew, G. H. (2020). Morphometric analysis for prioritizing sub-watersheds and management planning and practices in Gidabo Basin Southern Rift Valley of Ethiopia. *Applied Water Science*, *10*(7), 1–15
- Acharyya, S. K., & Ray, K. K. (1977). Geology of the Darjeeling–Sikkim Himalaya. Guide to Excursion No. 3. In *Fourth International Gondwana Symposium (Calcutta)*. Geological Survey of India (pp. 1–25).
- Akay, H., & Baduna Koçyiğit, M. (2020). Flash flood potential prioritization of sub-basins in an ungauged basin in Turkey using traditional multi-criteria decision-making methods. *Soft Computing*. <https://doi.org/10.1007/s00500-020-04792-0>
- Alkharabshah, M. M., Alexandridis, T. K., Bilas, G., Misopolinos, N., & Silleos, N. (2013). Impact of land cover change on soil erosion hazard in Northern Jordan using remote sensing and GIS. *Procedia Environmental Sciences*, *19*, 912–921. <https://doi.org/10.1016/j.proenv.2013.06.101>
- Altaf, S., Meraj, G., & Romshoo, S. A. (2014). Morphometry and land cover based multi-criteria analysis for assessing the soil erosion susceptibility of the western Himalayan watershed. *Environmental Monitoring and Assessment*, *186*(12), 8391–8412. <https://doi.org/10.1007/s10661-014-4012-2>
- Bhattacharya, R. K., Chatterjee, N. J., & Das, K. (2019). Multi-criteria-based sub-basin prioritization and its risk assessment of erosion susceptibility in Kansai-Kumari catchment area, India. *Applied Water Science*, *9*(76), 1–30. <https://doi.org/10.1007/s13201-012-0045-2>
- Borkar, V. S., Gokhale, N. B., More, S. S., Wahane, M. R., & Khobragade, N. H. (2018). Mapping land use/cover using remote sensing and GIS techniques: A case study of rahat micro watershed of Nagpur district India. *International Journal of Chemical Studies*, *6*(1), 15–18
- Chaubey, P. K., Srivastava, P. K., Gupta, A., et al. (2020). Integrated assessment of extreme events and hydrological responses of Indo-Nepal Gandak River Basin. *Environment, Development and Sustainability*. <https://doi.org/10.1007/s10668-020-00986-6>
- Chauhan, P., Chauniyal, D. D., Singh, N., & Tiwari, R. K. (2016). Quantitative geo-morphometric and land cover-based micro-watershed prioritization in the Tons river basin of the lesser Himalaya. *Environment and Earth Science*, *75*, 498. <https://doi.org/10.1007/s12665-016-5342-x>
- Chen, L., Qian, X., & Shi, Y. (2011). Critical area identification of potential soil loss in a typical watershed of the Three Gorges reservoir region. *Water Resources Management*, *25*(13), 3445–3463. Approach. *International Journal Geomat Geoscience*, *1*(3), 511–528. <https://doi.org/10.1007/s11269-011-9864-4>
- Choudhari, P. P., Nigam, G. K., Singh, S. K., & Thakur, S. (2018). Morphometric based prioritization of watershed for groundwater potential of Mula river basin, Maharashtra, India. *Geology, Ecology and Landscape*, *2*(3), 1–12. <https://doi.org/10.1080/24749508.2018.1452482>
- Dar, R. A., Chandra, R., & Romshoo, S. A. (2013). Morphotectonic and lithostratigraphic analysis of intermontane Karewa basin of Kashmir Himalayas India. *Journal of Mountain Science*, *10*(1), 1–15. <https://doi.org/10.1007/s11629-013-2494-y>
- Eniolorunda, N. B., & Ifabiyo, I. P. (2012). Watershed characteristics and their implication for hydrologic response in the upper Sokoto basin, Nigeria. *Journal of Geography and Geology*, *4*(2), 147. <https://doi.org/10.5539/jgg.v4n2p147>
- Farhan, Y., Anbar, A., Al-Shaikh, N., Almohammad, H., Alshawamreh, S., & Barghouthi, M. (2018). Prioritization of sub-watersheds in a large semi-arid drainage basin (Southern Jordan) using morphometric


- analysis, GIS, and multivariate statistics. *Agricultural Science*, 09(04), 437–468. <https://doi.org/10.4236/as.2018.94031>
- Fenta, A. A., Yasuda, H., Shimizu, K., Haregeweyn, N., & Woldearegay, K. (2017). Quantitative analysis and implications of drainage morphometry of the Agula watershed in the semi-arid northern Ethiopia. *Applied Water Science*, 7(7), 3825–3840. <https://doi.org/10.1007/s13201-017-0534-4>.
- Foody, G. M. (2002). Status of land cover classification accuracy assessment. *Remote Sensing of Environment*, 80(1), 185–201. [https://doi.org/10.1016/S0034-4257\(01\)00295-4](https://doi.org/10.1016/S0034-4257(01)00295-4)
- Grohmann, C. H. (2004). Morphometric analysis in geographic information systems: Applications of free software GRASS and R. *Computers & Geosciences*, 30(9–10), 1055–1067.
- Hembram, T. K., & Saha, S. (2020). Prioritization of sub-watersheds for soil erosion based on morphometric attributes using fuzzy AHP and compound factor in Jainti River basin, Jharkhand, Eastern India. *Environment, Development and Sustainability*, 22, 1241–1268. <https://doi.org/10.1007/s10668-018-0247-3>
- Horton, R. E. (1932). Drainage basin characteristics. *Transactions American Geophysical Union*, 13, 350–361. <https://doi.org/10.1029/TR013i001p00350>
- Horton, R. E. (1945). Erosional development of streams and their drainage basins: Hydrophysical approach to quantitative morphology. *Bulletin of the Geological Society of America*, 56, 275–370. [https://doi.org/10.1130/0016-7606\(1945\)56\[275:EDOSAT\]2.0.CO;2](https://doi.org/10.1130/0016-7606(1945)56[275:EDOSAT]2.0.CO;2)
<https://doi.org/10.1007/s13201-020-01239-7>
[https://doi.org/10.1130/0016-7606\(1952\)63\[1117:HAAOET\]2.0.CO;2](https://doi.org/10.1130/0016-7606(1952)63[1117:HAAOET]2.0.CO;2)
- Huggel, C. (2004). Assessment of glacial hazards based on remote sensing and GIS modeling Geographisches Institut der Universität Zürich in the semi-arid northern Ethiopia. *Applied Water Science*. <https://doi.org/10.1007/s13201-017-0534-4>
- Jaiswal, R. K., Ghosh, N. C., Galkate, R. V., & Thomas, T. (2015). Multi criteria decision analysis (MCDA) for watershed prioritization. *Aquat Procedia*, 4, 1553–1560. <https://doi.org/10.1016/j.aqpro.2015.02.201>
- Kavian, A., Azmoodeh, A., & Solaimani, K. (2014). Deforestation effects on soil properties, runoff and erosion in Northern Iran. *Arabian Journal of Geosciences*, 7(5), 1941–1950. <https://doi.org/10.1007/s12517-013-0853-1>
- Kolekar, S. S., Mishra, A., Choudhari, P., & Choudhari, N. R. (2021). Identification of specific areas for water conservation measures using Geoinformatics approach. *Arabian Journal of Geosciences*, 14(6), 1–13. <https://doi.org/10.1007/s12517-021-06721-3>
- Kulimushi, L. C., Choudhari, P., Mubalama, L. K., & Banswe, G. T. (2021). GIS and remote sensing-based assessment of soil erosion risk using RUSLE model in South-Kivu province, Eastern Democratic Republic of Congo. *Geomatics, Natural Hazards and Risks*,. <https://doi.org/10.1080/19475705.2021.1906759>
- Kumar, A., Jayappa, K., & Deepika, B. (2011). Prioritization of sub-basins based on geomorphology and morphometric analysis using remote sensing and geographic information system (GIS) techniques. *Geocarto International*, 26, 569–592. <https://doi.org/10.1080/10106049.2011.606925>
- McCloskey, J. T., Lilieholm, R. J., & Cronan, C. (2011). Using Bayesian belief networks to identify potential compatibilities and conflicts between development and landscape conservation. *Landscape and Urban Planning*, 101, 190–203. <https://doi.org/10.1016/j.landurbplan.2011.02.011>
- Meshram, S. G., Alvandi, E., Meshram, C., Kahya, E., & Fadhil Al-Quraishi, A. M. (2020). Application of SAW and TOPSIS in prioritizing watersheds. *Water Resources Management*, 34(2), 715–732. <https://doi.org/10.1007/s11269-019-02470-x>
- Miller, V. C. (1953). A quantitative geomorphic study of drainage basin characteristics in the Clinch mountain area Virginia and Tennessee (Proj. NR 389–402, Technical Report 3). New York, NY: Department of Geology, ONR, Columbia University, Virginia and Tennessee. Accession Number: AD0057755
- Montgomery, D. R., & Dietrich, W. E. (1992). Channel initiation and the problem of landscape scale. *Science*, 255(5046), 826–830.
- Morgan, R. P. C. (2009). *Soil erosion and conservation*. Wiley.
- Mosbahi, M., Benabdallah, S., & Boussema, M. R. (2013). Assessment of soil erosion risk using SWAT model. *Arabian Journal of Geosciences*, 6(10), 4011–4019. <https://doi.org/10.1007/s12517-012-0658-7>
- Nitheshnirmal, S., Thilagaraj, P., Abdul Rahaman, S., & Jegankumar, R. (2019). Erosion risk assessment through morphometric indices for prioritisation of Arjuna watershed using ALOS-PALSARDEM. *Modeling Earth Systems and Environment*. <https://doi.org/10.1007/s40808-019-00578-y>
- Nooka, R. K., Srivastava, Y. K., Venkateshwara Rao, V., Amminedu, E., & Murthy, K. S. R. (2005). Check dam positioning by prioritization of micro-watersheds using SYI model and morphometric

- analysis—remote Sensing and GIS perspective. *Journal of the Indian Society of Remote Sensing*, 33(1), 25–38. <https://doi.org/10.1007/BF02989988>
- Pal, S. (2016). Impact of Massanjore Dam on hydro-geomorphological modification of Mayurakshi River, Eastern India. *Environment, Development and Sustainability*, 18, 921–944. <https://doi.org/10.1007/s10668-015-9679-1>
- Pande, C. B., Moharir, K. N., Singh, S. K., Varade, A. M., Elbeltagi, A., Khadri, S. F. R., & Choudhari, P. (2021). Estimation of crop and forest biomass resources in a semi-arid region using satellite data and GIS. *Journal of the Saudi Society of Agricultural Sciences*. <https://doi.org/10.1016/j.jssas.2021.03.002> ISSN 1658-077X.
- Pham, T. G., Degener, J., & Kappas, M. (2018). Integrated universal soil loss equation (USLE) and Geographical Information System (GIS) for soil erosion estimation in A Sap basin: Central Vietnam. *International Soil and Water Conservation Research*, 6(2), 99–110. <https://doi.org/10.1016/j.iswcr.2018.01.001>
- Rahaman, S. A., Ajeez, S. A., Aruchamy, S., & Jegankumar, R. (2015). Prioritization of sub watershed based on morphometric characteristics using fuzzy analytical hierarchy process and geographical information system—a study of Kallar watershed. *Aquatic Procedia, Tamil Nadu*. <https://doi.org/10.1016/j.aqpro.2015.02.172>
- Rahmati, O., Samadi, M., Shahabi, H., Azareh, A., Rafiei-Sardooi, E., Alilou, H., & Shirzadi, A. (2019). SWPT: An automated GIS-based tool for prioritization of sub-watersheds based on morphometric and topo-hydrological factors. *Geoscience Frontiers*, 10(6), 2167–2175. <https://doi.org/10.1016/j.gsf.2019.03.009>
- Rudraiah, M., Govindaiah, S., & Vittala, S. S. (2008). Morphometry using remote sensing and GIS techniques in the sub-basins of Kagna river basin, Gulburga district, Karnataka, India. *Journal of the Indian Society of Remote Sensing*, 36(4), 351–360.
- Rushema, E., Maniragaba, A., Ndiokubwayo, L., & Kulimushi, L. C. (2020). The impact of land degradation on agricultural productivity in Nyabihu District-Rwanda. A Case Study of Rugera Sector. *International Journal of Environmental and Agriculture Research*, 6(7), 49–63s. <https://doi.org/10.5281/zenodo.3969676>
- Saghafian, B., Golian, S., Elmi, M., & Akhtari, R. (2013). Monte Carlo analysis of the effect of spatial distribution of storms on prioritization of flood source areas. *Natural Hazards*, 66, 1059–1071. <https://doi.org/10.1007/s11069-012-0537-2>
- Schumm, S. A. (1956). Evolution of drainage systems and slopes in Bad Lands at Perth Amboy, New Jersey. *Geological Society of America Bulletin*, 67, 597–646. [https://doi.org/10.1130/0016-7606\(1956\)67\[597:EODSAS\]2.0.CO;2](https://doi.org/10.1130/0016-7606(1956)67[597:EODSAS]2.0.CO;2)
- Sharma, S. K., Gajbhiye, S., Nema, R. K., Tignath S. (2015). Assessing Vulnerability to Soil erosion of a Watershed of Narmada basin using Remote Sensing and GIS International Journal of Science and Innovative Engineering and Technology 1. ISSN 978-81-904760-6-5
- Sharma, R., Sahai, B., & Karale, R. L. (1986). Identification of erosion-prone areas in a part of the Ukai catchment. In Asian Conference on Remote Sensing, 6 th, Hyderabad, India (pp. 121–126).
- Sheikh, V., Kornejady, A., & Ownegh, M. (2019). Application of the coupled TOPSIS–Mahalanobis distance for multi-hazard-based management of the target districts of the Golestan Province. *Iran Nat Hazards*, 96(3), 1335–1365. <https://doi.org/10.1007/s11069-019-03617-0>
- Singh, P., Thakur, J. K., & Singh, U. C. (2013). Morphometric analysis of Morar River Basin, Madhya Pradesh, India, using remote sensing and GIS techniques. *Environmental Earth Sciences*, 68(7), 1967–1977. <https://doi.org/10.1007/s12665-012-1884-8>
- Smith, K. G. (1950). Standards for grading texture of erosional topography. *American Journal of Science*, 248(9), 655–668. <https://doi.org/10.2475/ajs.248.9.655>
- Sreedevi, P. D., Owais, S. H. H. K., Khan, H. H., & Ahmed, S. (2009). Morphometric analysis of a watershed of South India using SRTM data and GIS. *Journal of the Geological Society of India*, 73(4), 543–552
- Strahler, A. N. (1952). Hypsometric (area-altitude) analysis of erosional topography. *Bulletin of the Geological Society of America*, 63, 1117–1142
- Strahler, A. N. (1957). Quantitative analysis of watershed geomorphology. *Eos, Transactions American Geophysical Union*, 38(6), 913–920. <https://doi.org/10.1029/TR038i006p00913>
- Strahler, A. N. (1964). *Part II. Quantitative geomorphology of drainage basins and channel networks*. (pp. 4–39). Handbook of Applied Hydrology: McGraw-Hill, New York.
- Tamang, D. K., Dhakal, D., Shresta, D. G., & Sharma, N. P. (2012). Morphometric analysis and prioritization of miniwatersheds in Rongli watershed, Sikkim (India) using remote sensing and GIS techniques. *International Journal of Fundamental and Applied Sciences*, 1(3), 61–66

- Todorovski, L., & Džeroski, S. (2006). Integrating knowledge driven and data-driven approaches to modeling. *Ecological Modelling*, 194(1), 3–13. <https://doi.org/10.1016/j.ecolmodel.2005.10.001>
- Trabucchi, M., Comín, F. A., & O'Farrell, P. J. (2013). Hierarchical priority setting for restoration in a watershed in NE Spain based, on assessments of soil erosion and ecosystem services. *Regional Environmental Change*. <https://doi.org/10.1007/s10113-012-0392-4>
- Tripathi, M. P., Panda, R. K., & Raghuvanshi, N. S. (2003). Identification and prioritisation of critical sub-watersheds for soil conservation management using the SWAT model. *Biosystems Engineering*, 85(3), 365–379. [https://doi.org/10.1016/S1537-5110\(03\)00066-7](https://doi.org/10.1016/S1537-5110(03)00066-7)
- Uwemeye, J., Nsanzumukiza, M. V., Maniragaba, A., Ndaruhutse, T., Kulimushi, L. C., Harera, E., & Mucyo, J. C. (2020). Role of local community in Gishwati forest reserve rehabilitation and its implication on local community livelihood. *American Journal of Environment and Sustainable Development*, 5(3), 43–51
- Vittala, S. S., Govindiah, S., & Honne Gowda, H. (2004). Morphometric analysis of sub-watersheds in the pawagada area of Tumkur district, South India, using remote sensing and GIS techniques. *Journal of the Indian Society of Remote Sensing*, 32, 351–362. <https://doi.org/10.1007/BF03030860>
- Wadadar, S. (2016). Morphometric analysis of the Lachung River Basin, North Sikkim India. *Asian Journal of Multidisciplinary Studies*, 4(10), 67–73
- Yadav, S. K., Singh, S. K., Gupta, M., & Srivastava, P. K. (2014). Morphometric analysis of Upper Tons basin from Northern Foreland of Peninsular India using CARTOSAT satellite and GIS. *Geocarto International*, 29(8), 895–914. <https://doi.org/10.1080/10106049.2013.868043>

Publisher's Note Springer Nature remains neutral with regard to jurisdictional claims in published maps and institutional affiliations.

Authors and Affiliations

Paolenmang Haokip¹  · Md. Abdullah Khan¹ · Pandurang Choudhari²  ·
Luc Cimusa Kulimushi³ · Ibodullo Qaraev⁴

Paolenmang Haokip
haokiplen12@gmail.com

Md. Abdullah Khan
akhan@cus.ac.in

Luc Cimusa Kulimushi
kcimusa@gmail.com

Ibodullo Qaraev
ibodullo_93@list.ru

¹ Department of Geology, Sikkim University, Gangtok, Sikkim, India

² Department of Geography, University of Mumbai, Mumbai, India

³ Faculty of Environmental Studies, University of Lay Adventists of Kigali, Kigali Campus, P.O. Box: 6392, Kigali, Rwanda

⁴ Aerospace Information Research Institute (AIR), University of Chinese Academy of Sciences (CAS), Dengzhuang Suth Road, Haidian District, Beijing District, China